Conditions for self-collimation in three-dimensional photonic crystals

Jonghwa Shin and Shanhui Fan

Department of Electrical Engineering, Stanford University, Stanford, California 94305

Received March 11, 2005; accepted April 28, 2005

We introduce the theoretical criterion for achieving three-dimensional self-collimation of light in a photonic crystal. Based on this criterion, we numerically demonstrate a body-center-cubic structure that supports wide-angle self-collimation and is directly compatible with the recently developed holographic fabrication technique. We further show that both bends and beam splitters can be introduced into this structure by the use of interfaces. © 2005 Optical Society of America

OCIS codes: 130.2790, 160.3130.

Recently there has been impressive progress in synthesizing three-dimensional (3D) photonic crystal structures at optical length scales with self-assembly[1,2] or holographic inscription[3–6] techniques. However, it still remains a challenge to create functional integrated photonics circuits in 3D crystals by using these techniques.[7] While the designs of basic components, including waveguides, bends, and splitters, have relied exclusively on the use of controlled line defect states[8–10] in a 3D photonic bandgap, self-assembly or holographic inscription appears to be particularly suitable for creating large-scale *periodic* structures.[1–6]

In this Letter we show that a periodic 3D crystal structure alone, without any line defects, may also be used to achieve functionalities of integrated photonic circuits. Our approach is based on the self-collimation effect.[11–18] We prove rigorously that, in a 3D crystal, a self-collimation k point can be created if the structure possesses certain symmetry properties. We also present empirical considerations with respect to enlarging the k-space area over which self-collimation occurs. Based on these considerations, we present a structure that exhibits true 3D self-collimation and can be fabricated with the holographic technique.

First, we consider the mathematical conditions for creating a self-collimation point in the wave-vector space for a 3D crystal. At such a point, the radius of curvature of the constant-frequency surface (CFS) is infinite along every possible tangential direction. In general, the CFS around a k point $\mathbf{k}_0=(k_{x0},k_{y0},k_{z0})$ can be described in terms of a Taylor series:

$$\begin{aligned} k_z = f(k_x,k_y) = {} & f(k_{x0},k_{y0}) + \left.\frac{\partial f}{\partial k_x}\right|_{k_{x0},k_{y0}} (k_x-k_{x0}) \\ & + \left.\frac{\partial f}{\partial k_y}\right|_{k_{x0},k_{y0}} (k_y-k_{y0}) + \left.\frac{1}{2}\frac{\partial^2 f}{\partial k_x^2}\right|_{k_{x0},k_{y0}} (k_x-k_{x0})^2 \\ & + \left.\frac{\partial^2 f}{\partial k_x\,\partial k_y}\right|_{k_{x0},k_{y0}} (k_x-k_{x0})(k_y-k_{y0}) \\ & + \left.\frac{1}{2}\frac{\partial^2 f}{\partial k_y^2}\right|_{k_{x0},k_{y0}} (k_y-k_{y0})^2 + \cdots . \end{aligned} \tag{1}$$

Without losing generality we can choose the z direction as the direction of group velocity for this k point; then the first-order terms in Eq. (1) are identically zero. At a self-collimation point, the second-order terms in Eq. (1) must be identically zero as well. This can be accomplished if the structure has threefold or higher rotational symmetry around the z axis and the radius of curvature is infinite along at least one tangential direction. To see this, we note that the radius of curvature $R_{\hat{u}}$ along an arbitrary tangential direction $\hat{u}=\hat{x}\cos\theta+\hat{y}\sin\theta$ can be expressed in terms of second-order derivatives:

$$\begin{aligned} R_{\hat{u}} = \frac{1}{\partial^2 f/\partial u^2} = 2/[&(A+C)+(A-C)\cos(2\theta) \\ &+ 2B\sin(2\theta)], \end{aligned} \tag{2}$$

where

$$A=\frac{\partial^2 f}{\partial k_x^2},\quad B=\frac{\partial^2 f}{\partial k_x\,\partial k_y},\quad C=\frac{\partial^2 f}{\partial k_y^2}.$$

Thus, if the radius of curvature is infinite along at least one tangential direction, the threefold or sixfold rotational symmetry guarantees that the radius of curvature is infinite along at least three nonparallel directions. Alternatively, if the structure has fourfold rotational symmetry around the z axis, we have at least two nonparallel directions along which the radius of curvature is infinite, and the symmetry further dictates that B is zero. In either case, A, B, and C are identically zero, and $\mathbf{k}_0$ becomes a self-collimation point.

Most of the photonic crystals with threefold or higher rotational symmetry have a frequency extremum point, in addition to Γ, that lies on a symmetry axis at least for some bands, and therefore possess a self-collimation point. For practical applications, however, it is also important to have a broad, flat area on the CFS around the self-collimation point.

0146-9592/05/182397-3/$15.00

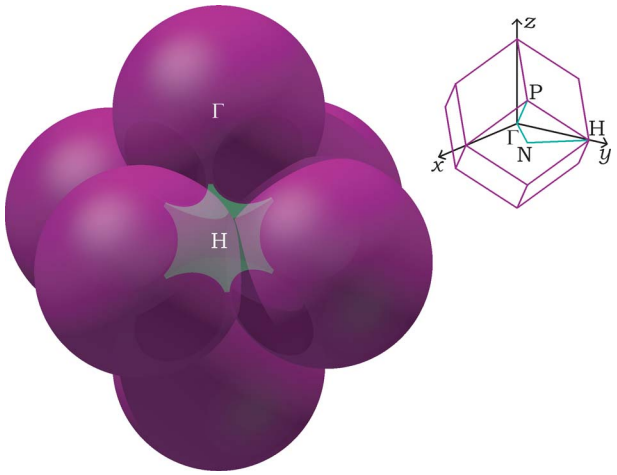

Fig. 1. Constant-frequency surface (CSF) around the H point for an empty BCC lattice. The inset shows the first Brillouin zone.

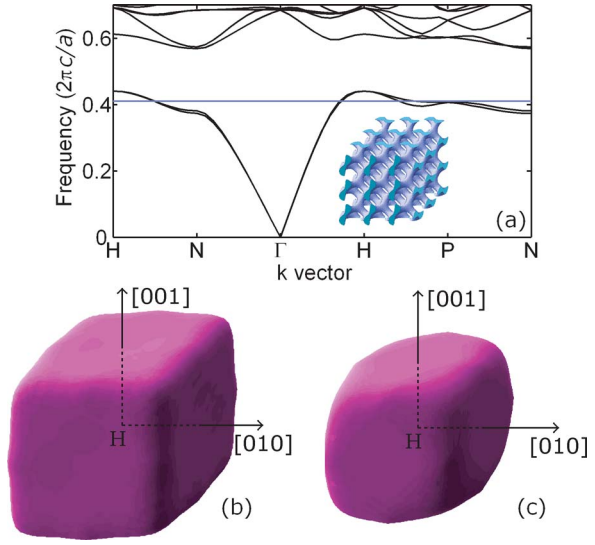

Fig. 2. (a) Band structure of a BCC gyroid crystal. The crystal is plotted in the inset. The horizontal line indicates the position of the frequency of 0.41 ($2\pi c/a$). (b), (c) Calculated constant frequency surface around the H point at frequencies (b) 0.40 ($2\pi c/a$), (c) 0.41 ($2\pi c/a$).

Since a lower band has a lower normalized frequency, the radius of the constant frequency sphere in air is smaller, and the angle of acceptance is larger. That makes body-centered-cubic (BCC) structures good candidates. In a BCC lattice, the [100] direction has fourfold rotational symmetry. Moreover, the first-band frequency maximum is typically located at the H point ([100] direction), since H is the farthest point in the first Brillouin zone. Therefore there is a self-collimation point on the Γ–H line. In addition, for each H point there are only six nearby surrounding Γ points; the CFS around the H point therefore resembles a cube, with only six faces (Fig. 1). Assuming the same enclosed volume, the individual flat regions of the CFS are larger than what they might have been if the CFS had had 8 or 12 faces.

Here, we use a BCC gyroid structure similar to that in Refs. 5 and 6, created with six modulations along all ⟨110⟩ directions, since such a structure possesses a large symmetry group. The structure is defined by

$$\epsilon(x,y,z) = 12.06 \quad \text{if} \quad \sin(2\pi(x+y)/a) + \sin(2\pi(x-y)/a) + \sin(2\pi(y+z)/a) + \sin(2\pi(y-z)/a) + \sin(2\pi(z+x)/a) + \sin(2\pi(z-x)/a) > 2.0,$$

$$\epsilon(x,y,z) = 1 \text{ otherwise}, \tag{3}$$

where a is the length of the cubic unit cell. This structure has a filling ratio of 17%. A band structure calculation[19] shows a 25% bandgap between the second and third bands [Fig. 2(a)]. (Experimentally, there has been much effort toward infiltrating high-index materials into holographically defined templates.[3]) In the vicinity of frequency $0.41 \times 2\pi c/a$, the structure exhibits a very flat CFS around an H point that resembles the aforementioned cubical surface [Figs. 2(b) and 2(c)]. Compared with bulk silicon, this structure has less longitudinal wavenumber variation up to a lateral wavenumber of $0.14 \times 2\pi/a$, and that corresponds to an approximately 20° angle for light incident from air.

Simulation by the finite-difference time-domain method[20] further demonstrates the self-collimating nature of the beam inside the structure [Fig. 3(a)]. We use large samples to minimize the effect of boundary reflection, $30 \times 30 \times 50$ unit cells for straight propagation and larger for bends and splitters. The source is located at $1a$ outside of the structure, is linearly polarized, and has a Gaussian profile with a beam waist radius of $2a$ and a frequency of $0.41 \times 2\pi c/a$. (The use of linearly polarized light excites both the first and the second bands.) Over a propagation distance of $50a$, the beam size does not show significant variation. In comparison, for the same input beam, the Gaussian beam radius at the end of propagation will grow to $5.9a$ in bulk silicon.

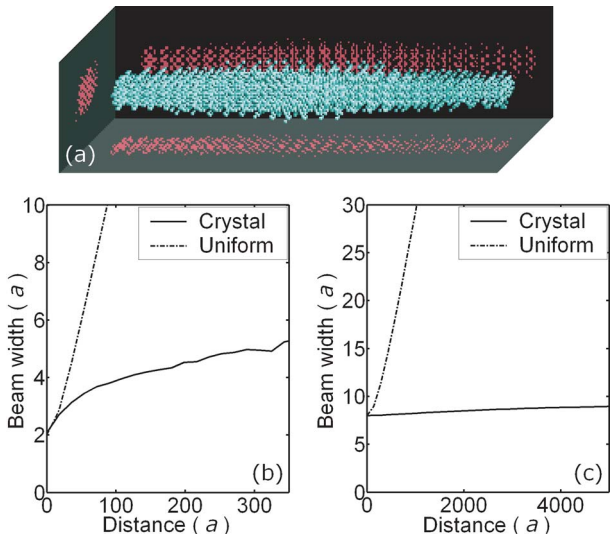

Fig. 3. (a) Propagation of a self-collimated beam, with an initial beam radius of $2a$ as calculated in a finite-difference time-domain simulation. Shown here is the intensity of the electric field. (b), (c) Beam width as a function of propagation distance for an initial beam radius of (b) $2a$ and (c) $8a$.

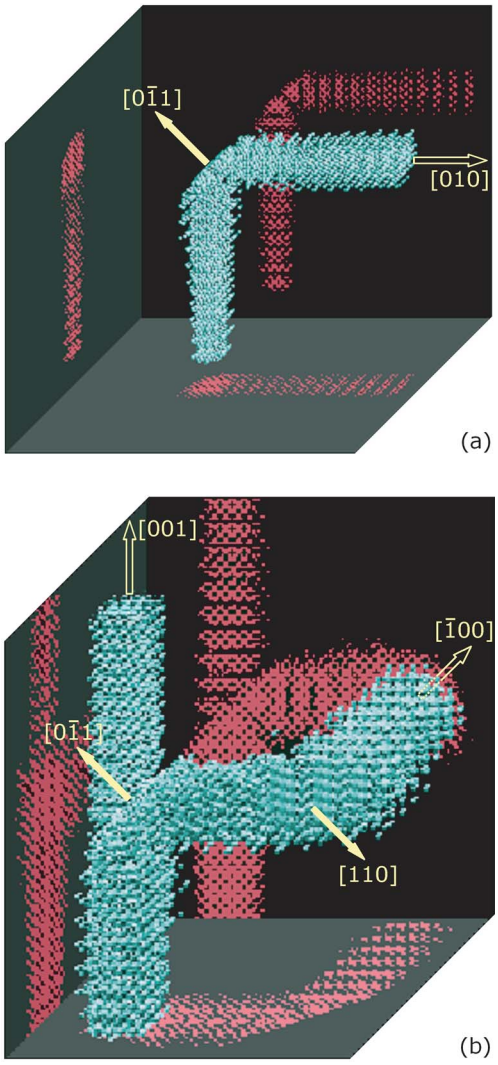

Fig. 4. Intensity plot as a light beam goes through (a) a 90° bend, (b) a splitter and then a bend. Filled arrows, normal direction of interfaces; open arrows, propagation direction.

To visualize the beam divergence over longer distances, for which the finite-difference time-domain method is not well suited owing to its heavy computational requirement, we instead use an approximate method based on the CFS. For the calculation, a Gaussian input beam is decomposed into its transverse wave vector components. The output beam is then constructed by summing all components, each multiplied by an appropriate phase factor calculated from the CFS and the propagation distance. (This method assumes an angle-independent coupling ratio at the interface, so it can be less accurate for short distances.) After a propagation distance of $360a$, the beam radius of the self-collimated beam remains below $5.5a$, while that of the beam propagating in uniform silicon increases to $40a$ [Fig. 3(b)]. For larger initial widths, the improvement over uniform medium becomes even more dramatic [Fig. 3(c)].

A mirror for the self-collimated beam can be constructed simply by truncating the crystal in a (011) plane. In this case, a beam along the [001] direction incident upon the truncation will undergo total internal reflection, since the projection of the wave vector on the surface lies outside the k sphere of air. Based on this, a 90° bend for a self-collimated beam is easily realized, and the bending efficiency is nearly complete [Fig. 4(a)]. Furthermore, by cascading two of such truncations, one can create a beam splitter. This is shown in Fig. 4(b), in which the distance between the two truncations is $0.15\sqrt{2}a$, with air between the two surfaces. The power efficiency to each of the two ports is approximately 48% at the frequency of $0.41 \times 2\pi c/a$. These calculations demonstrate that functional integrated optical components can indeed be constructed in 3D photonic crystals without the use of line defects.

The work is supported in part by Department of Defense Multidisciplinary University Research Initiative (ARO-MURI) grant DAAD19-03-1-0227. The simulations were performed through the support of a National Science Foundation National Resource Allocation Committee (NSF-NRAC) program. J. Shin (joshin@stanford.edu) also acknowledges a Samsung Lee Kun Hee Scholarship.

References

1. P. V. Braun and P. Wiltzius, Nature **402**, 603 (1999).
2. Y. A. Vlasov, X. Z. Bo, J. C. Sturm, and D. J. Norris, Nature **414**, 289 (2001).
3. M. Campbell, D. N. Sharp, M. T. Harrison, R. G. Denning, and A. J. Turberfield, Nature **404**, 53 (2000).
4. L. Z. Cai, X. L. Yang, and Y. R. Wang, Opt. Lett. **27**, 900 (2002).
5. O. Toader, T. Y. M. Chan, and S. John, Phys. Rev. Lett. **92**, 043905 (2004).
6. C. K. Ullal, M. Maldovan, E. L. Thomas, G. Chen, Y. Han, and S. Yang, Appl. Phys. Lett. **84**, 5434 (2004).
7. W. Lee, S. A. Pruzinsky, and P. V. Braun, Adv. Mater. (Weinheim, Ger.) **14**, 271 (2002).
8. A. Chutinan and S. Noda, Appl. Phys. Lett. **75**, 3739 (1999).
9. M. Povinelli, S. G. Johnson, S. Fan, and J. D. Joannopoulos, Phys. Rev. B **64**, 075313 (2003).
10. A. Chutinan, S. John, and O. Toader, Phys. Rev. Lett. **90**, 123901 (2003).
11. R. Zengerle, J. Mod. Opt. **34**, 1589 (1987).
12. H. Kosaka, T. Kawashima, A. Tomita, M. Notomi, T. Tamamura, T. Sato, and S. Kawakami, Appl. Phys. Lett. **74**, 1212 (1999).
13. M. Notomi, Phys. Rev. B **62**, 10696 (2000).
14. J. Witzens, M. Loncar, and A. Scherer, IEEE J. Sel. Top. Quantum Electron. **8**, 1246 (2002).
15. J. Witzens and A. Scherer, J. Opt. Soc. Am. A **20**, 935 (2003).
16. X. Yu and S. Fan, Appl. Phys. Lett. **83**, 3251 (2003).
17. L. Wu, M. Mazilu, and T. F. Krauss, J. Lightwave Technol. **21**, 561 (2003).
18. C. Chen, A. Sharkawy, D. M. Pustai, S. Shi, and D. W. Prather, Opt. Express **11**, 3153 (2003).
19. S. G. Johnson and J. D. Joannopoulos, Opt. Express **8**, 173 (2001).
20. K. S. Kunz and R. J. Luebbers, *The Finite-Difference Time-Domain Methods for Electromagnetics* (CRC Press, 1993).